Physica B 652 (2023) 414612

Contents lists available at ScienceDirect

Physica B: Condensed Matter

journal homepage: www.elsevier.com/locate/physb

Doping effects on minority carrier parameters in bulk GaAs

S. Ilahi [a,b]

[a] Laboratoire de Recherche de Caractérisation Photo-thermique, IPEIN, 8000, Nabeul, Université de Carthage, Tunisia
[b] Université de Monastir, Faculté des Sciences de Monastir, Département de Physique, Tunisia

ARTICLE INFO

Keywords:
Non-radiative lifetime
GaAs diffusion length
Surface and interface recombination velocity
Bulk GaAs

ABSTRACT

In this paper, we measured the experimental amplitude and phase of the Photothermal deflection signal for bulk GaAs "silicon" doped n + type, "chromium" doped n type and "carbon" doped p type in order to determine the nonradiative recombination parameters. The results obtained for non-radiative lifetime and the electronic diffusion agree with those appearing in the literature for similar samples. By comparison with values reported in literature, the increase of doping density favors auger recombination that produce an increase of non-radiative lifetime. We have found that electron mobility in p type *C*-doped GaAs is about 300 $cm^2/V{\cdot}s$. In fact, holes motilities are respectively 177 and 193 $cm^2/V{\cdot}s$ for n + type Si-doped GaAs and n type Cr-GaAs doped. However, we obtained high values of the recombination velocity for non passivated surface.

1. Introduction

Technological advances in various fields such as communication, medicine, on-board electronics are based on the development of new micro and optoelectronic components. Thus, improving the performance of these components based on semiconductor materials requires knowledge and investigation of transport properties. In this context and more specifically, the gallium arsenide material GaAs is experiencing considerable growth leading to real technological leaps in microelectronics and optoelectronics, citing the manufacture of solid-state detectors [1], high efficiency [2], infrared LEDs [3], lasers [4] and diodes [5]. Indeed, for the improvement of the performances and the quality of GaAs material, it is necessary to investigate their electronic properties such as non-radiative lifetime, the electronic diffusivity and the surface recombination velocity. Photothermal technique is non-destructive, known for its high sensitivity and commonly used for determining the optical and thermal properties of semiconductors [6–10]. On the other hand, the use of Photothermal techniques to study transport properties in semiconductors has recently experienced renewed high interest [11–20]. The transport parameters determination is infer using laborious theoretical models that take into account heat diffusion and photo-generated carriers equations. Historically, the first theoretical model was developed by A. Rosencwaig in 1973 [16] for photoacoustic detection technique. This model based on the acoustic technique describes the origin of the sound wave detected by a high sensitivity microphone. However, in 1990 the transport properties in the GaAs semiconductor were studied for the first time by A. Pinto Neto et al. [17] using the photoacoustic technique. In 1981, A.C Boccara et al. [18] introduced a new Photothermal technique based on the detection of the thermal wave by prospecting the index gradient induced by the variation in temperature gradient of the fluid in contact with the surface of the sample, the technique used then took the name photothermal detection or "Mirage Effect". In 1986, the study of transport properties in semiconductors was carried out for the first time by D. Fournier et al. [19] using the thermal photo deflection technique (PTD). This study is carried out using a theoretical model based on solving the diffusion equations of minority carriers and heat. Thus, by adjusting the experimental curves to the theoretical one derived from the model, they were able to determine the thermal diffusivity, the non-radiative lifetime, the electronic diffusion coefficient and the recombination velocity at the surface for a bulk sample of silicon. In addition, there has been a renewed interest in studying the electronic properties of semiconductors by the mirage effect technique. Recently, A.R Warrier et al. **[20]** improved the model proposed by D. Fournier to determine the transport parameters in the thin layers of CuInS2, SnS and β-In_2S_3. However, their model does not take into account the diffusion of carriers, which concern only to the case of thin semi-conducting layers deposited on an insulating substrate. Thus, the model proposed by S. Ilahi et al. [15] remains more general because it takes into consideration the diffusion of heat and minority carrier diffusion. Specifically, this model is mainly relative to the case of bulk semiconductors. For bulk semiconductors such as GaAs, InP, InSb and GaSb, which present high thermal conductivity respectively around 68, 27 and 32 W/m.K [21–23], which are advantageous for optoelectronic devices leading to dissipate heat as possible.

E-mail address: soufiene.ilehi@fsm.rnu.tn.

https://doi.org/10.1016/j.physb.2022.414612
Received 21 November 2022; Received in revised form 21 December 2022; Accepted 23 December 2022
Available online 5 January 2023

One of the explanation is traduced by that thermal conductivity depends in materials thickness and phonon scattering in bulk materials, in most cases, thermal conductivity in thick material is higher than ternary and quaternary semiconductors layers [24]. More precisely, GaAs material known as good candidate due to sharp interfaces as well as a good lattice matching between the layer and the substrate. For this raison, the GaAs is used as a substrate for based vertical-cavity surface-emitting lasers (VCSELs) at 1,3–1,55 μm wavelength emission [25,26] and for multi-jonction solar cells [27,28].

2. Theoretical model

As illustrates in Fig. 1, a laser beam irradiates the surface of the sample. The photothermal effect occurs when absorbed light energy that generate a thermal wave that propagate into the sample and surrounding media. Subsequently, the propagation of the vibration of phonons or electrons causes heat transfer. In fact, heat energy is provided by non-radiative recombination process that occurs in semiconductors sample. Three heats sources are identified: surface recombination, bulk recombination and carrier thermalization. The presented model is describe in details elsewhere [14,15], in which incident light is assumed to be uniform. It means that one-dimensional treatment of the thermal wave is sufficient. The theory is based on coupling of thermal and minority carrier diffusion equations.

One dimensional heat diffusion equation in the different media is written as (Fig. 1):

$$\frac{\partial^2 T_f}{\partial x^2} - \sigma_f^2 T_f = 0 \quad \text{if} \quad 0 \le x \le l_f \tag{1}$$

$$\frac{\partial^2 T_s}{\partial x^2} - \sigma_s^2 T_s = Q_{(x,t)} \quad \text{if} - l \le x \le 0 \tag{2}$$

$$\frac{\partial^2 T_b}{\partial x^2} - \sigma_b^2 T_b = 0 \quad \text{if} - l_b - l \le x \le -l \tag{3}$$

Where $\sigma_i = \frac{(1+i)}{\mu_i}$ and $\mu_i = \left(\frac{D_i}{\pi F}\right)^{1/2}$ is the thermal diffusion length of the i medium (i = f, s,b respectively the fluid f, the sample s and the backing b), and F is the modulation frequency of the pump beam

$Q_{(x,t)}$ represents the heat source term which is the sum of three contributions [14]: $Q_{th(x,t)} = \alpha I_0 (1-R)\left(\frac{\Delta E}{E}\right)\exp(\alpha x)$ reflects the carriers thermalization, I_0 is the intensity of pump beam, α is the optical absorption coefficient,R is the reflectivity coefficient and E is the energy of the incident beam. $\Delta E = E - E_g$ is the excess energy by interaction with phonons in the crystal lattice.

$Q_{bulk(x,t)} = \frac{-E_g}{\tau K_s} N_{(x,t)}$ is due by the bulk recombination of photo-generated carriers. $Q_{Sur(x,t)} = S\, E_g N_{(x,t)}$ represents the recombination at sample surface. Where S is the surface recombination velocity and $N_{(x,t)}$ is the photogenerated carriers density obtained by resolving the minority carrier equation.

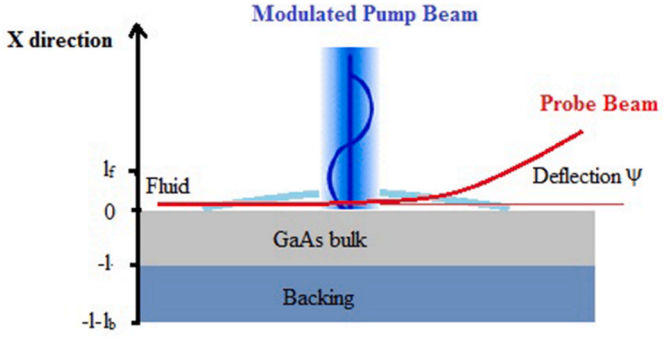

Fig. 1. Schematic descriptive of PTD technique Principle.

$\frac{\partial N_{(x,t)}}{\partial t} = D\frac{\partial^2 N_{(x,t)}}{\partial x^2} - \frac{N_{(x,t)}}{\tau} + G$ Where $N_{(x,t)}$ is the photo-generated carriers density, D the electronic diffusion coefficient and (τ_{nr}) is the non-radiative lifetime of minority carriers and $G = \frac{\alpha I_0 (1-R)}{2E}\exp(\alpha x)$ is the generation rate carriers. I_0 is the intensity of pump beam, α is the optical absorption coefficient,R is the reflectivity coefficient and E is the energy of the incident beam.

After heat equation resolution, we obtained the expression of the periodic temperature rise at the sample surface T_0 by taking into account of boundary condition of temperature and heat transfer. This expression is detailed in Ref. [14].

$$T_0 = \frac{\left\{\begin{array}{l}(1-f)\exp(-\sigma_s x)\left[m(1+a_s)+n(1-a_s)+(r+1)(q+A)-\frac{SE_g}{K_s\sigma_s}N(0)\right] \\ -(1+f)\exp(\sigma_s x)\left[m(1-a_s)+n(1+a_s)+(1-r)(q+A)+\frac{SE_g}{K_s\sigma_s}N(0)\right] \\ +2m(f-a_s)\exp(-al)+2n(f+a_s)\exp(+al)+2(q+A)(f-r)\exp(-\alpha l)\end{array}\right\}}{[(1-f)(1-g)\exp(-\sigma_s l)-(1+f)(1+g)\exp(\sigma_s l)]} \tag{15}$$

The expression of probe beam deflexion is written as:

$\psi = \frac{L}{n}\frac{dn}{dT}\sigma_f T_0 \exp(-\sigma_f x_0)$, ψ is complex number that we can written as $\psi = |\psi|\exp(\varphi)$ where $|\psi|$ is the amplitude and φ the phase of PTD signal

3. Experimental setup

The PTD experimental setup is presented in detail elsewhere [11–13], where a mechanically chopped light illuminates the sample by halogen lamp (250 w). The laser probe beam is He–Ne laser type that presents a wavelength of 632 nm (10 mW) with diameter of 1 mm of diameter 100 μm grazing the sample surface is deflected. This deflection is detected by a position photodetector, related to a lock in amplifier. A computer connected to lock-in amplifier permits to read the experimental data of amplitude and phase as a function of square root modulation frequency.

The growth of GaAs bulk is performed by molecular beam epitaxy **[10]**. The study is performed to three samples: GaAs "n+" Si-doped type, GaAs "n" Cr-doped type and GaAs "p" type *C*-doped.

4. Results and discussions

The fitting procedure is based on a least-squares method. In order to ensure the uniqueness issue of the fitted values, the details of multiparameters fitting is similar with that described by us [11–15]. We have determined the mean square variance for each parameter. In the analyses, in order to minimize the mean square variance, the simulated PTD data are fitted with expression (15) by fixing one transport parameter to different values and keeping the other three as free parameters in the multi-parameter fitting procedure. Indeed, optical and thermal parameters of the sample, the fluid and the support, which are used for the simulation, are recorded in Table 1.

Table 1
Thermal, optical properties of GaAs, backing and fluid.

	GaAs Si-doped	GaAs Cr-doped	GaAs*C* -doped	Air	Backing
Gap Energy (eV) [29]	1,4	1,4	1,4	–	–
Doping density N (cm^{-3})	2×10^{18}	4×10^{17}	5×10^{17}	–	–
Thickness l (μm)	420	450	505	–	–
Thermal Conductivity (W/m/K) [30]	45	45	45	0,02	0,1
Thermal Diffusivity (m^2/s) [30]	$0,25 \times 10^{-4}$	$0,25 \times 10^{-4}$	$0,25 \times 10^{-4}$	2	0,02

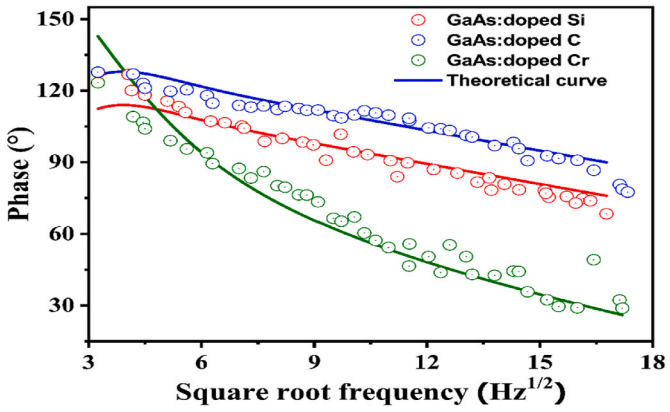

Fig. 2. Exper\imental normalized amplitudes of PTD signal and the corresponding theoretical ones versus square root frequency of doped bulk GaAs samples.

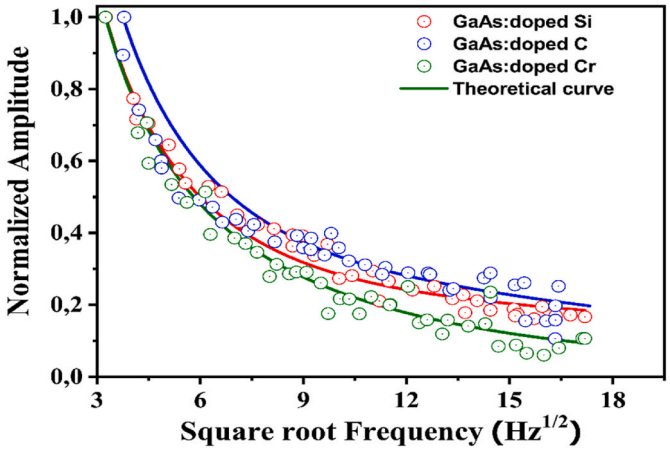

Fig. 3. Experimental phases of PTD signal and the corresponding theoretical ones versus square root frequency of doped bulk GaAs samples.

Figs. 2 and 3 represent respectively the variations of the experimental amplitudes and phases as a function of the square root of the modulation frequency of the PTD signal with those corresponding theoretical ones for doped GaAs samples. In fact, we discuss the values obtained for each electronic parameter by the photo-thermal detection technique compared with those appearing in the literature. In fact, the present electronic parameters found for the three structures Si-doped "n+" type GaAs, Cr-doped "n" type GaAs and *C*-doped "p" type GaAs are given in the table below.

5. Non-radiative lifetime

The values of the non-radiative lifetime measured by the PTD technique for the three samples of GaAs doped C, Cr and Si are listed in Table 2. For comparison, a difference between the values that we measured and those reported by others techniques such as photoacoustic technique. Non radiative lifetime values for p + type Be doped GaAs, semi-insulating n doped GaAs and heavily "n+" Si doped are of the order of a few μs [17,31,32]. On the other hand, for p + type GaAs doped carbon is of the order of ns [33], whereas the values obtained for GaAs doped Si, Cr, C are respectively 4,3 × 10^{-8} s and 5 × 10^{-8}s and 3,1 × 10^{-7}s. This difference between is generally explained by defect density in the material [31], which depends on several factors citing the growth technique, the type of dopant [34,35] or the density doping [31].

According to the recombination types, the non-radiative lifetime is composed of two types. Traps recombination, namely as Shokely-Red-Hall (SRH) recombination [37]. This kind of recombination is related to traps levels that depend on the density of impurities and deep vacancies, which act as centers of non-radiative recombination for the photo-generated carriers. The second type of recombination is Auger-recombination, which describes the interaction between the photo-generated carriers and the crystal lattice (phonon) in the semiconductor. Auger recombination is related to doping density [24,38,39]. The expression of non-radiative recombination is written as follow: $\frac{1}{\tau_{nr}} = \frac{1}{\tau_{SRH}} + \frac{1}{\tau_{Auger}}$ where τ_{SRH} is the Shockley-Read-Hall (SRH) lifetime and τ Auger is the Auger lifetime.

SRH recombination becomes more predominant if the doping density is less than 10^{18} cm^{-3} [39]. Therefore, the Auger recombination is most probably negligible for the Cr and C doped GaAs samples. On the other hand, Auger recombination depends essentially on the doping density. This type of recombination occurs when the doping density is greater than 10^{18} cm^{-3} [30,38,39]. In our case, the SRH recombination will be negligible for the GaAs sample heavily doped Si "n+". It is worth to mention that U. Strauss et al. [29] demonstrate the effect of doping density on the Auger lifetime. They measured the Auger lifetime for Carbon-doped GaAs sample for different doping densities. They found that the Auger lifetime increases from 20 ps to 30 ps by varying the doping density from 3,4 × 10^{18} cm^{-3} to 8 × 10^{18} cm^{-3} [31]. This study explain well the difference between our present value for GaAs p type *C*-doped and that published by Maassdof et al. [33,36] for p + *C*-doped GaAs. Indeed, S.D.George et al. [31] presented the best value of p + type Be-doped GaAs that reaches 5 μs, which is the more suitable for optoelectronics.

For n type GaAs, our present values is higher than that reported in literature [31,32] that reflects the high density of defects in GaAs materials, which is undesirable for optoelectronics applications .

6. Electronic diffusion coefficient

The electronic diffusion coefficient that expressed in cm^2/s describes the movement of the carriers and represent a curial parameter for minority carrier mobility and diffusion length determination. Indeed, the

Table 2
Electronic parameters of different doped GaAs bulk.

Present result for GaAs p type	GaAs p: C doped	τ(s)	D (m^2/s)	S (cm/s)
		3,1 10^{-7} (±7,8%)	7,99 × 10^{-4} (±1%)	153 (25%)
Results published by A. Maaβdorf et al. [33,36].	GaAs p^+: C doped	1,6 × 10^{-9}	6 × 10^{-5}	14,000
Results published by S. D. George et al. [31]	GaAs p^+: Be doped	5 × 10^{-6}	5,6 × 10^{-4}	634
	GaAs n^+: Si doped	**4,3 × 10^{-8} (±11,24%)**	**4,6 *10^{-4} (± 3,2%)**	**7942 (± 1,6%)**
Present results for GaAs n type	**GaAs n: Cr doped**	**5 × 10^{-8} (±14,32%)**	**5* 10^{-4} (± 0,14%)**	**100 (±0,1%)**
Results published by S.D.George et al. [31]	GaAs n^+: Si doped	7 × 10^{-6}	4,5 × 10^{-4}	525
Results published by A.P. Neto et al. [17]	GaAs n: Si doped	6,05 × 10^{-6}	9,10 × 10^{-4}	580,7
Results published by P.M.Nikolic et al. [32]	GaAs dopé n: semi-insulating	2,7 × 10^{-6}	4,3 × 10^{-4}	583

study of electronic diffusion coefficient is necessary for the production of laser and heterojunction bipolar transistors [40]. Furthermore, the values of the electron diffusion coefficient for the three C, Cr and Si doped GaAs samples are presented in Table 2. The found electron diffusion coefficients are in good agreement with those mentioned in the literature [17,23,24]. The slight variation of the diffusion coefficient existing between different types of GaAs samples is attributed to the type and density of doping [20,41,42]. Thus, a study [43] shows that the electronic diffusion coefficient of p-type Zn-doped GaAs decreases with increasing doping density. According to doping types and carrier mobility, the electronic diffusion coefficient for n-type samples is generally larger than that of GaAs p-type [31].

7. Mobility and diffusion length of minority carrier

GaAs material has tremendous advantages, including ideal direct band gap, good radiation resistance, low temperature coefficient and high conversion efficiency. As well know, GaAs contain high densities of localized energy states or generation-recombination centers, which has a strong effect on the characteristics of many semiconductor devices. The non-radiative recombination has a profound effect on the performance of optoelectronics devices such as a solar cell and diode laser. Indeed, the mobility of minority carrier is deduced through the Einstein relation $\mu = Dq/K_bT$ n b where D, q, K_b, and T are respectively, electronics diffusion coefficient, Boltzmann constant, charge and temperature. The determination of diffusion length L_n and mobility of minority carrier μ_n is crucial and give an information about layer quality. We have found that electron mobility in p type *C*-doped GaAs is about 300 cm^2/V·s. In fact, holes motilities are respectively 177 and 193 cm^2/V·s for n + type Si-doped GaAs and n type Cr-GaAs doped. In fact, C. M. Colomb et al. [44] expect a continual decrease in minority electron mobility with increasing p-type doping. In contrast, our result agree well with several studies, which reveal that minority electron mobility increase as respect of doping density. This behavior is explained by plasmon scattering reduction and the Pauli Exclusion Principle [45]. Accordingly, a theoretical prediction that attribute the increase in minority electron mobility in p + GaAs to reductions in plasmon and carrier-carrier scattering at high hole densities [46].

Carrier diffusion length is another crucial parameter for the modeling and optimization of modern devices and for quality evaluation of optoelectronics devices [47,48]. Knowing the non-radiative lifetime τ and the electronic scattering coefficient D allows us to determine the electronic scattering length through the relation $L_n = \sqrt{\tau D}$. We compared the electron scattering lengths L obtained for three samples of GaAs doped with C, Cr and Si with that appearing in the literature. Indeed, the values that have been calculated are of the order of 5 (±7%) μm for the Cr-doped GaAs and 5 (±4,4%) μm for the *C*-doped GaAs which are in good agreement with the value appearing in the literature [49] which is 6,3 μm. On the other hand, for the Si-doped n + type GaAs, the diffusion length is of the order of 1,42 μm (±7,2%). The difference between the values is due to the doping density [50]. As a result, H. Casey et al. **[50]** showed that the scattering length decreases from 7 μm to 0,8 μm for a doping concentration of 10^{16} cm^{-3} and 10^{19} cm^{-3} respectively. Furthermore, the same effect of doping density on electron scattering length is demonstrated for a sample of Mg-doped p-type GaN. Thus, L decreases from 950 nm to 220 nm by increasing the doping density from 4×10^{18} cm^{-3} to 3×10^{19} cm^{-3} [48].

8. Surface recombination velocity

The surface recombination velocity of semiconductors is a measure of the recombination rate of minority carriers at the sample surface. The determination of this parameter is of great interest in optoelectronics and photovoltaic fields [51]. Indeed, the values of the recombination rate at the surface that were measured by the PTD technique for the three samples of GaAs doped C, Cr and Si are listed in Table 2. Consequently, a slight variation of the values of the recombination velocity at the surface of the samples Si-doped n + type GaAs is 525 m/s [31], Be-doped p + type GaAs is 634 m/s [36] and the semi-insulating GaAs is of the order of 580 m/s [17,43]. On the other hand, for p + type GaAs doped carbon, the surface recombination velocity is 14,000 m/s [33], whereas the values obtained for GaAs doped Si, Cr, C are respectively 7942 m/s, 100 m/s and 153 m/s. Indeed, the values presented provide us with information on the density of the defects. The difference between the present values and those reported in literature using photoacoustic technique. This discrepancy is explained by non-passivated surfaces in which recombination rate varies randomly because it depends on the surface state of the sample. Indeed, contaminations, surface defects and broken chemical bonds are the main causes of the increase in the recombination rate of minority carriers [36,32,42]. This explain why semiconductors surface undergo special treatments (passivation) [49, 52] to limit the rate of recombination of photo-generated carriers. Indeed, the majority of LED diodes and GaAs-based lasers are developed by epitaxial techniques such as the molecular beam epitaxy technique [42,43], which usually leads to obtain high quality materials with low defect densities.

9. Conclusion

In Summary, we have determined the electronic parameters i.e. the non-radiative lifetime, the electronic diffusion coefficient and the recombination velocity at the surface of bulk samples Si-doped n + type GaAs, Cr-doped n-type GaAs and GaAs *C*-doped p-type. Then, the extraction of these parameters is done by adjusting the theoretical curves to the experimental ones. It was found that the results found are acceptable and in good agreement with those appearing in the literature. Surface recombination velocity varies randomly that can be found around of 7942 m/s, 100 m/s and 153 m/s GaAs doped Si, Cr, C respectively. However, the obtained values of minority carrier lifetime for GaAs doped Si, Cr, C are respectively $4{,}3 \times 10^{-8}$ s and 5×10^{-8}s and $3{,}1 \times 10^{-7}$s.Accordinagly, the diffusion length of minority carrier is around of 5 (±7%), 5 (±4,4%) and 1.42 μm (±7,2%) for the Cr, C and Si doped GaAs respectively. Further, we have found that electron mobility in p type *C*-doped GaAs is about 300 cm^2/V·s. In fact, holes motilities are respectively 177 and 193 cm^2/V·s for n + type Si-doped GaAs and n type Cr-GaAs doped.

Credit author statement

S.ILAHI: Investigation Conceptualization Methodology, Software, Validation. Formal analysis, Visualization, Writing – original draft, Writing – review & editing.

Declaration of competing interest

The authors declare that they have no known competing financial interests or personal relationships that could have appeared to influence the work reported in this paper.

Data availability

Data will be made available on request.

References

[1] J.E. Eberhardt, R.D. Ryan, A.J. Tavendale, Nucl. Instrum. Methods 94 (1971) 463–476.
[2] K. Nakayama, K. Tanabe, H.A. Atwater, Appl. Phys. Lett. (2008), 93121904.
[3] F.K. Yam, Z. Hassan, J. Microelectron. 36 (2005) 129–137.
[4] Huiyun Liu, Ting Wang, Qi Jiang, Richard Hogg, Tutu Frank, Francesca pozzi and alwyn seeds, Nat. Photonics 5 (2011) 416–419.
[5] S.J.J. Teng, R.E. Goldwasser, IEEE Electron. Device Lett. 10 (1989) 412–414.

[6] A. Khalfaoui, S. Ilahi, M. Abdel-Rahman, M.F. Zia, M. Alduraibi, B. Ilahi, Phys. B Condens. Matter 522 (26–30) (2017).
[7] S. Ilahi, N. Yacoubi, F. Genty, Opt. Mater. 69 (2017) 226–229.
[8] D. Loubiri, Z.B. Hamed, S. Ilahi, Sanhoury Ma, F. Kouki, N Yacoubi Synthetic Metals 206 (2015) 1–7.
[9] S. Ilahi, F. Saidi, R. Hamila, N. Yacoubi, H. Maaref, B. L Auvray Physica, Condensed Matter 421 (2013) 105–109.
[10] S. Abroug, F. Saadallah, F. Genty, N. Yacoubi Physics Procedia 2 (2009) 787–795.
[11] S. Ilahi, M. Baira, F. Saidi, N. Yacoubi, H. L Auvray, Maaref Journal of alloys and compounds 581 (2013) 358–362.
[12] S. Ilahi, N. Yacoubi, F. Genty, Mater. Res. Bull. 106 (2018) 332–336.
[13] S. Ilahi, C. Cornet, N. Yacoubi, O. Durand, Sol. Energy Mater. Sol. Cell. 215 (2020), 110622.
[14] S. Ilahi, N Yacoubi Semiconductors 48 (3) (2014) 302–306.
[15] S. Ilahi, F. Saadalah, N. Yacoubi, Appl. Phys. A 110 (2013) 459–464.
[16] A. Rosencwaig, Opt Commun. 7 (1973) 305–308.
[17] A. Pinto Neto, H. Vargas, N.F. Leite, L.C.M. Miranda, Phys. Rev. B 41 (1990) 9971–9979.
[18] A.C. Boccara, D. Fournier, J. Badoz, Appl. Phys. Lett. 36 (1980) 130–132.
[19] D. Fournier, C. Boccara, A. Skumanich, N.M. Amer, J. Appl. Phys. 59 (1986) 787–795.
[20] A.R. Warrier, T.H. Sajeesh, C.S. Kartha, K.P. Vijayakumar, Mater. Res. Bull. 47 (2012) 3758–3763.
[21] S. Adachi, J. Appl. Phys. 102 (2007), 063502.
[22] V.M. Glazov, K. Davletov, A. Ya Nashelskii, M.M. Mamedov, Zh. Fiz. Khim. 51 (10) (1977) 2558–2561.
[23] A.S. Okhotin, A.S. Pushkarskii, V.V. Gorbachev, Thermophysical Properties of Semiconductors, Atom" Publ. House, Moscow, 1972.
[24] P.S. Dutta, H.L. Bhat Vikram Kumar, J. Appl. Phys. 81 (9) (1997).
[25] John F. Klem, Darwin K. Serkland, O. Blum, Kent M. Geib, A.W. Jackson, R. L. Naone, J.M. Dalberth, J. Smith . Electronics Letters 36 (11) (2000) 951–952.
[26] Christyves Chevallier, Frédéric Genty, Nicolas Fressengeas, Joël Jacquet, J. Lightwave Technol. 31 (21) (2013) 3374–3380.
[27] Tatsuya Takamoto, Minoru Kaneiwa, Mitsuru Imaizumi, Masafumi Yamaguchi Photovoltaics 13 (2005) 6.
[28] P.P. NayakJ, P. DuttaG, P. Mishra, Engineering Science and Technology 18 (3) (2015) 325–335.
[29] Y. Sayad, Thesis « Détermination de la longueur de diffusion des porteurs de charges minoritaires dans le silicium cristallin par intéraction lumière matière », 2009 SAL 0053.
[30] R. Jeremiah, Lowney and herbert S. Bennett J, Appl. Phys. 69 (1991) 7102, https://doi.org/10.1063/1.347650.
[31] S. George, P. Suresh Kumar, P. Radhakrishnan, V.P.N. Nampoori, C.P.G. Vallabhan, Proc. SPIE-Int. Soc. Opt. Eng. (2002) 4918.
[32] P.M. Nikolic, D.M. Todorovic, A.I. Bojicic, K.T. Radulovic, D. Urosevic, J. Elazar, V. Blagojevic, P. Mihajlovic, M. Miletic, J. Phys. Condens. Matter 8 (1996) 5673.
[33] A. Maaßdorf, S. Gramlich, E. Richter, F. Brunner, M. Weyers, G. Tränkle, J. Appl. Phys. 91 (2002) 5072–5078.
[34] L. Hernández, D. Seuret, O. Vigil, Cryst. Res. Technol. 17 (1982) K12–K16.
[35] R.J. Nelson, R.G. Sobers, J. Appl. Phys. 49 (1978) 6103–6108.
[36] Koki Saito, Eisuke Tokumitsu, Takeshi Akatsuka, Motoya Miyauchi, Takumi Yamada, Makoto Konagai, Kiyoshi Takahashi, J. Appl. Phys. 64 (1988) 3975–3979.
[37] W. Shockley, W.T. Read, Phys. Rev. 87 (1952) 835–842.
[38] C.M. Colomb, S.A. Stockman, N.F. Gardner, A. P.-Curtis, G.E. Stillman, T.S. Low, D. E. Mars, D.B. Davito, J. Appl. Phys. 73 (1993) 7471.
[39] E.S. Harmon, M.L. Lovejoy, M.R. Melloch, M.S. Lundstrom, T.J. de Lyon, J. M, Woodall Citation: Appl. Phys. Lett. 63 (1993) 536.
[40] G. Stollwerck, O.V. Sulima, A.W. Bett, IEEE trans, Electron Devices 47 (2000) 448–457.
[41] W. Nakwaski, J. Appl. Phys. 64 (1988) 159–166.
[42] M.A. Tischler, T.F. Kuech, MRS Online Proc. Libr. Arch. 144 (1988).
[43] L. Hernández, D. Seuret, O. Vigil, Cryst. Res. Technol. 17 (1982) K12–K16.
[44] R.J. Nelson, R.G. Sobers, J. Appl. Phys. 49 (1978) 6103–6108.
[45] N. Nordell, P. Ojala, W.H. van Berlo, G. Landgren, M.K. Linnarsson, J. Appl. Phys. 67 (1990) 778–786.
[46] L. Hernández, D. Seuret, O. Vigil, Cryst. Res. Technol. 17 (1982) K12-K16.
[47] K. Kumakura, T. Makimoto, N. Kobayashi, T. Hashizume, T. Fukui, H. Hasegawa, Appl. Phys. Lett. 86 (2005), 052105.
[48] H.H. Lee, R.J. Racicot, S.H. Lee, Appl. Phys. Lett. 54 (1989) 724–726.
[49] H.C. Casey, B.I. Miller, E. Pinkas, J. Appl. Phys. 44 (1973) 1281–1287.
[50] Y. Da, Y. Xuan, Opt Express 21 (2013) A1065–A1077.
[51] E.Y. Chang, G.T. Cibuzar, K.P. Pande, IEEE Trans. Electron. Dev. 35 (1988) 1412–1418.
[52] C.A. Wang, J. Cryst. Growth 170 (1997) 725–731.